

**SCATTERING BY A DIELECTRIC CYLINDER
FOR SEABED LOGGING
A MATHEMATICAL MODELING APPROACH**

by

Gerhana Sasongko Supendi

Project dissertation submitted in partial fulfillment of
the requirements for the
Bachelor of Engineering (Hons)
(Electrical and Electronic Engineering)

JUNE 2009

Universiti Teknologi PETRONAS

Bandar Seri Iskandar

31750 Tronoh

Perak Darul Ridzuan

CERTIFICATION OF APPROVAL

SCATTERING BY A DIELECTRIC CYLINDER FOR SEABED LOGGING A MATHEMATICAL MODELING APPROACH

by

Gerhana Sasongko Supendi

A project dissertation submitted to the
Electrical & Electronics Engineering Faculty
Universiti Teknologi PETRONAS
in partial fulfillment of the requirement for the
Bachelor of Engineering (Hons.)
(Electrical & Electronic Engineering)

Approved by,



(Puan Azizah Zainal Abidin)

UNIVERSITI TEKNOLOGI PETRONAS

TRONOH, PERAK

June 2009

CERTIFICATION OF ORIGINALITY

This is to certify that I am responsible for the work submitted in this project, that the original work is my own except as specified in the references and acknowledgements, and that the original work contained herein have not been undertaken or done by unspecified sources or persons.



Gerhana Sasongko Supendi

ABSTRACT

A method of predicting hydrocarbon reservoirs by using seismic survey and analysis has been implemented over decades. This method has shown pretty good approach of locating the presence of hydrocarbon layer especially in vertical dimension (thick well). The problem is that this method is not quite suitable for locating the hydrocarbon layer in lateral dimension (thin layer). Engineers came up with technique called Seabed Logging to complete the technique. It uses the fact that the hydrocarbon layer has much higher resistivity than its surroundings. The objective of this Final Year Project is to study and simulate one way of doing Seabed Logging by analyzing the direct wave and the scattered wave from the hydrocarbon layer. An Oil and Gas Journal by Statoil published in 2002 is studied and referred as the main source. A solution of scattering by dielectric cylinder of arbitrary cross section shape published by Jack H. Richmond in his IEEE Transactions on Antennas and Propagation journal is also employed. Mathematical model is used as approximation since it is difficult and expensive to do experiment or to get the exact complete data of reservoir maps and structures. The scope of this project is limited to combining these techniques to calculate the direct wave and the wave scattered from the hydrocarbon layer modeled as dielectric cylinder. By working inversely, the signal received from the antennas is analyzed to yield information about the characteristics of the seabed and the hydrocarbon layer. The contrast between the hydrocarbon layer (relatively high resistivity) and seabed (relatively low resistivity) gives different wave responses and provides information of the presence of hydrocarbon reservoir beneath seabed. Combining the seismic technique and Seabed Logging would yield a higher preciseness in predicting and locating the presence of hydrocarbon reservoirs and thus reducing the costs of drilling uneconomical or dried well.

ACKNOWLEDGEMENTS

Praise be to Allah, The Most Gracious and The Most Merciful for His endless blessings throughout my life and the success. He has been guiding and granting me during my undergraduate studies and this final year project.

My utmost appreciation and gratitude is towards my supervisor Puan Azizan Zainal Abidin for her guidance throughout my final year project. Her knowledge, experience and support were very much helpful in passing so many obstacles, doubts and challenge that I faced. The trust she had on me kept me on track off the works and pushed me forward towards achieving my goals. I much thank Mr. Azizuddin bin Abdul Aziz and Puan Hanita Daud for giving me the journals as my bright starting point and all the lecturers who helped and gave me valuable support of knowledge and problem solving.

My appreciation is also extended to my family members, especially my mother and my father, for their continuous support and sincere prayers. Special thanks to Gizara Sugihartono for her supports throughout the years to believe in me and to make me believe in my self that I can reach my dreams. I thank Mr. Gunawan a lot for his brilliant ideas and solutions. Last but not least, I thank my friends, especially the International Students of EE graduating years 2009, and everyone else who encouraged and supported me throughout these four years of undergraduate studies and this final year project.

TABLE OF CONTENTS

ABSTRACT	iv
ACKNOWLEDGEMENT	v
LIST OF FIGURES	viii
LIST OF ABBREVIATION	x
CHAPTER 1: INTRODUCTION	1
1.1 Background of Study	1
1.2 Problem Statement	2
1.3 Objectives and Scope of Study	3
CHAPTER 2: LITERATURE REVIEW	4
2.1 Seabed Logging	4
2.2 Electromagnetic Wave Scattering by Dielectric Cylinder of Arbitrary Cross Section Shape	10
CHAPTER 3: METHODOLOGY	19
3.1 Project Flow Chart	19
3.2 Procedure Identification	22
3.3 Tools and Equipments.....	23
CHAPTER 4: RESULTS AND DISCUSSION	24
4.1 Results	24
4.2 Discussion	28
CHAPTER 5: CONCLUSION AND RECOMMENDATION..	31
5.1 Conclusion	31
5.2 Recommendation.....	32

REFERENCES	33
APPENDICES	35

LIST OF FIGURE

Figure 1	Simple model of seabed logging technique	7
Figure 2	EM wave in Seabed Logging technique	6
Figure 3	Cross section of a dielectric cylinder	9
Figure 4	The cross section of the dielectric cylinder is divided into small cells	16
Figure 5	Flow chart of Final Year Project	19
Figure 6	Flow chart of analysis of wave	20
Figure 7	Flow chart of complex wave number	21
Figure 8	Flow chart of electric of direct wave	21
Figure 9	Flow chart of direct wave signal magnitude	21
Figure 10	Flow chart of waveguide	22
Figure 11	Flow chart of refracted signal	22
Figure 12	Attenuation versus frequency	24
Figure 13	Electric field versus distance	25
Figure 14	Magnitude of direct wave versus distance	26
Figure 15	Direct wave attenuation	26
Figure 16	Waveguide wave number	27

Figure 17	Refracted wave signal	28
Figure 18	Contrast between direct and refracted waves	30
Figure 19	GUI for Seabed Logging simulation	45

LIST OF ABBREVIATION

CSEM	Controlled Source Electromagnetic
EM	Electromagnetic
HED	Horizontal Electric Dipole
TE	Transverse Electric
TM	Transverse Magnetic
TEM	Transverse Electromagnetic
GUI	Graphical User interface

CHAPTER 1

INTRODUCTION

1.1 Background of Study

Seismic survey and analysis has been implemented over decades to predict the presence of hydrocarbon layer under ground or soil layer, dessert, even deep down beneath seabed. Engineers have been using this method because it shows quite precise approximation of the structures of the material. The seismic also provides valuable information for mapping the location of hydrocarbon reservoir especially in vertical direction (thick well). However, this method is not quite suitable for locating the hydrocarbon layer in lateral dimension (thin layer).

A recently-developed technique called Seabed Logging has been widely discussed and promising a good approximation of predicting the presence of hydrocarbon layer underneath the seabed and mapping its structure in lateral dimension. It is a remote resistivity sensing method which employs the fact that the hydrocarbons have high resistivity (resistors) and thus the hydrocarbon-filled reservoirs have normally much higher than surrounding water-filled sediments.^[1] Some oil and gas company such as Statoil and Shell has been doing research and experiments of Seabed Logging and this method yields quite promising results. The technique can be combined with the seismic data to yield a better method of locating and mapping the hydrocarbon reservoirs.

In Seabed Logging, low frequency electromagnetic (EM) wave is used to avoid the high attenuation. The EM wave is transmitted from Horizontal Electric Dipole (HED) transmitter antenna through the seawater, seabed, and hydrocarbon layer (if present). Identical receiver antennas are installed on the sea floor to capture

the signal received directly from the HED transmitter as well as reflected from the seabed including the hydrocarbon layer. The contrast between the hydrocarbon layer (relatively high resistivity) and seabed (relatively low resistivity) shows the different wave response and provides the information of the presence of hydrocarbon reservoir beneath seabed.

1.2 Problem Statement

Seismic technique gives benefits to map the structure of hydrocarbon reservoir in vertical direction (detecting thick layer). However, this method is not suitable for mapping in lateral dimension (thin layer). Seabed Logging technique is developed to complete the method in predicting and locating the presence of hydrocarbon reservoir underneath the seabed. It is, however, quite expensive and difficult to do experiment and to get the complete data of hydrocarbon reservoir for the results and analyzing the preciseness of the methods. To overcome this, mathematical modeling is used to approximate the system.

The significance of this project is that Seabed Logging yields promising results in increasing the preciseness of predicting and locating the hydrocarbon reservoirs, especially when combined with the data received from the seismic technique. Thus, oil companies would reduce the possibility of drilling uneconomical or dried well and the production cost is reduced as well.

The relatively-high-resistive hydrocarbon layer is modeled as a dielectric cylinder and the signal scattered from this layer is analyzed using the Jack H. Richmond's scattering by dielectric cylinder method. Richmond set up a brilliant foundation in his theory in solving the problem of scattering by dielectric cylinder. Many scholars developed theories and solutions based on Richmond's model because it agrees with exact solution of scattering by dielectric cylinder. The technique is completed with the analysis of the direct wave received from the HED transmitter to give information about the characteristics of the hydrocarbon layer.

1.3 Objective and Scope of Study

The objective of this Final Year Project is to study and simulate one way of doing Seabed Logging. The hydrocarbon layer is modeled as a dielectric cylinder. The scattered wave from the hydrocarbon layer is analyzed using Jack H. Richmond's solution of scattering by dielectric cylinder of arbitrary cross section shape. As explained in his IEEE Transactions on Antennas and Propagation journal, the technique is valuable for calculating the scattering fields of dielectric cylinder of arbitrary cross section shape, completing other available solutions for the electromagnetic wave scattering by homogeneous or inhomogeneous cylinders of other shapes with finite cross section dimensions.^[2] The wave received directly from the HED transmitter is calculated using the method as explained in the Oil and Gas Journal published in 2002 by Kong F.N, et al from Statoil.

Concerning the time constrains, the scope of this project is limited to combining these techniques to calculate the direct wave and the wave scattered from the hydrocarbon layer. Some less dominant parameters such as the signal reflected from the air wave and from the seabed, the degree of the saturation of the hydrocarbon, and others are omitted. By working inversely, the signal received from the antennas is analyzed to yield information about the characteristics of the seabed and the hydrocarbon layer.

CHAPTER 2

LITERATURE REVIEW

2.1 Seabed Logging

Seabed Logging is another name for controlled source electromagnetic (CSEM) technique to determine the presence and extent of hydrocarbon reservoir beneath the seafloor.^[3] This technique has recently been discussed and developed to complete the other method by using seismic technique and survey. While seismic provides good results in mapping the hydrocarbon reservoir in vertical dimension, the Seabed Logging is suitable to mapping in lateral dimension.

Seabed Logging is a remote resistivity sensing method which exploits the fact that hydrocarbon filled reservoirs normally are electric insulator (or dielectric) and more resistive than surrounding water filled sediments.^[1] It uses a dipole source of electromagnetic wave that is towed just above the seafloor. It transmits a time-varying electromagnetic field into the sea environment and the field is then modified by the presence of subsurface resistive layers. These changes are detected and logged by an array of receivers placed on the sea floor. Thus, engineers would be able to determine the location of oil and gas by interpreting the behavior of the reflected and refracted waves received by the receivers.

Figure 1, courtesy of Statoil, Norwegian Geotechnical Institute, Oslo and Electromagnetic Geoservices AS Trondheim, Norway, below illustrates a simple model of seabed logging.^[1]

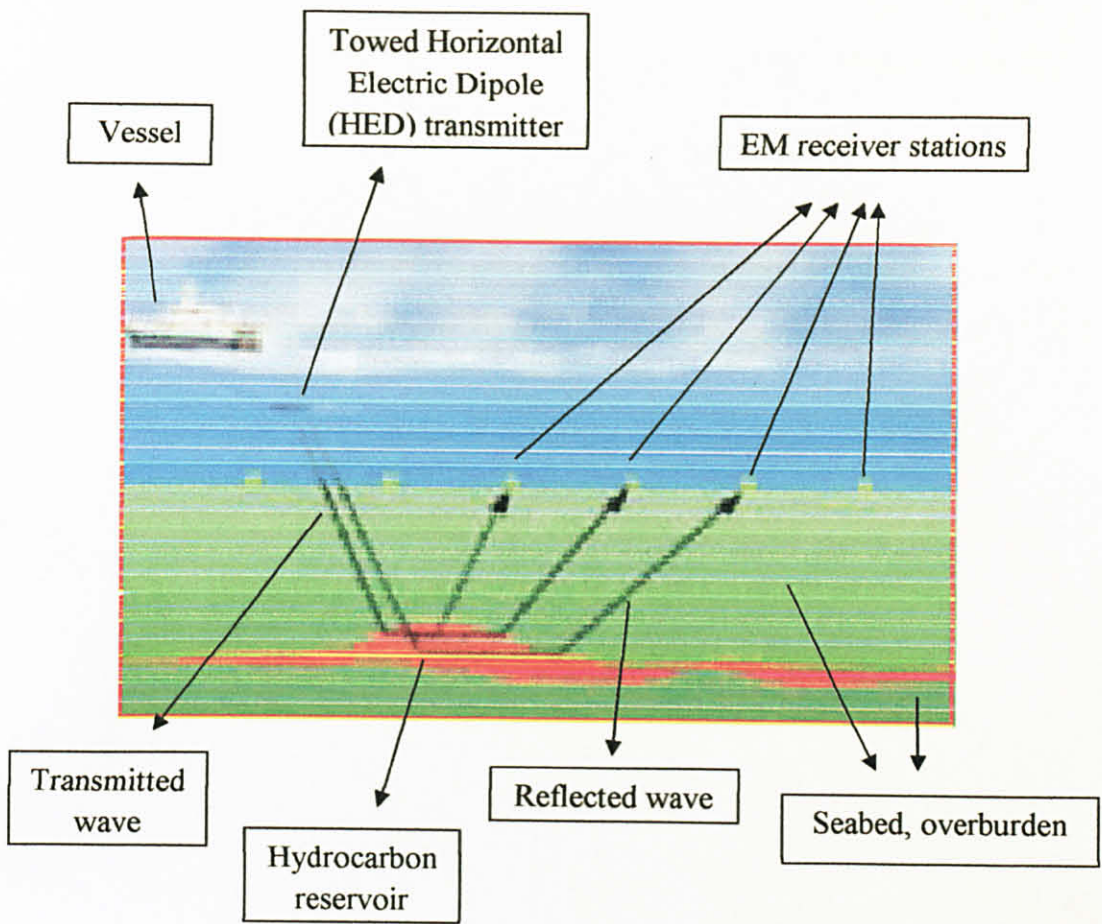


Figure 1. Simple model of seabed logging technique

A dipole (electric dipole) is a pair of equal charges of opposite signs that are very close together.^[4] The distance separating the two points is small compared to the distance to the point where we want to know the electric and potential fields. Electric field is a vector quantity that relates the force exerted on a charge to the size of the charge.^[5] It is the ratio of force and electric charge. It can be expressed in ratio of voltage over length or distance.

Seabed logging uses a very low frequency of EM wave, transmitted by Horizontal Electric Dipole (HED) transmitter antenna. The range can be from 0.1 Hz up to 10 Hz. EM wave propagates in three different modes: Transverse Electric (TE), Transverse Magnetic (TM) and also Transverse Electromagnetic (TEM). TE Mode has the characteristic of having electric field in z-direction (E_z) equal to zero while the magnetic field in z-direction (H_z) not equal to zero. TM mode has E_z not equal to zero and H_z equal to zero. TEM mode has both E_z and H_z equal to zero. The

modes act differently to a resistive hydrocarbon layer and these properties are used in acquiring the data for seabed logging.^[1]

An array of receivers is installed on the sea floor to capture the signal received directly from the HED transmitter as well as reflected from the seabed including the hydrocarbon layer. Figure 2 below shows the transmitted and received waves.

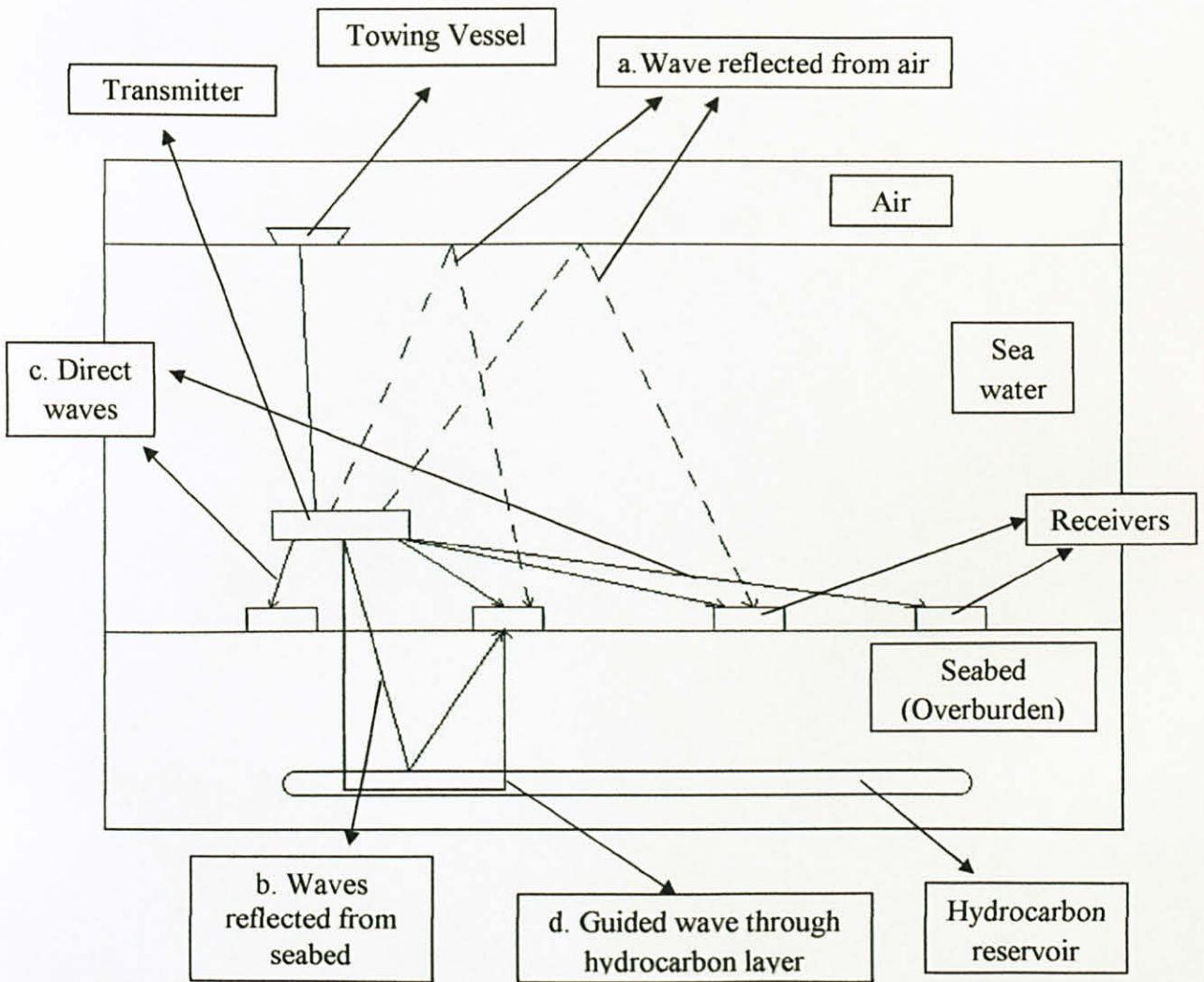


Figure 2. EM wave in Seabed Logging technique

Note that there are actually four (a, b, c and d) main waves to be received by the receiver. The wave reflected by the air (a) could be omitted in the deep sea analysis, since the distance travel to the water surface and back to the receiver is

long. The wave which travels longer distance through the seabed (b) has more attenuation than the guided wave which travels to and refracted from the hydrocarbon layer (d). The direct wave (c) is the wave received by the receivers directly from the transmitter. Equation of complex wave number ^[1] below would show the contrast of behavior of a sinusoidal plane EM wave between two different resistivity levels (seabed and hydrocarbon layer).

$$\mathbf{k} = \omega \sqrt{[\mu_0(\epsilon + j/(R*\omega))]} \quad (1)$$

where k = wave number

$$\omega = \text{angular frequency (rad/s)} = 2\pi f$$

$$f = \text{frequency (Hz)}$$

$$\mu_0 = \text{magnetic permeability}$$

$$\epsilon = \text{dielectric permittivity}$$

$$R = \text{electric resistivity } (\Omega)$$

The result is expected to be in form of $\alpha + j \beta$, where α is the phase constant (used to determine the velocity) and β is the attenuation constant.

The electric field of the direct wave transmitted directly from the transmitter to the receiver can be measured in the area where the receiver antennas are installed. The radial electric field along the antenna direction in the sea water nearby the sea floor at radial distance is calculated by the equation below. ^[1]

$$E_{\rho} = I * L_t * e^{jk} * ((1/\rho^3) - (j * k/\rho^2) - (k^2/\rho)) / (2 * \pi * \sigma_{sea}) \quad (2)$$

Where E_{ρ} = Electric field along the antenna direction (V/m)

$$I = \text{transmitter current (A)}$$

L_t = HED transmitter antenna effective length (m)

$$e^{jk} = \cos(k) + j \sin(k)$$

k = complex wave number of seabed (overburden layer)

ρ = radial distance from HED transmitter antenna

σ_{sea} = electric conductivity of the sea water (S/m)

Then, the signal magnitude of the direct wave can be calculated with the equation below. ^[1]

$$V_{dr} = I \cdot L_r \cdot L_t \cdot e^{jk} \cdot ((1/\rho^3) - (j \cdot k/\rho^2) - (k^2/\rho)) / (2 \cdot \pi \cdot \sigma_{sea}) \quad (3)$$

Where V_{dr} = Signal magnitude of the direct wave (V)

L_r = receiver antenna effective length (m)

Since the seabed has higher conductivity than the hydrocarbon layer, the hydrocarbon layer can be considered as a rectangular wave guide. According to the wave guide theory, ^[6] the wave number in z-direction (k_z) is calculated with the formula below. ^[1]

$$k_z = \sqrt{(k^2 - (m \cdot \pi/a)^2 - (n \cdot \pi/a)^2)} \quad (4)$$

Where m, n = integer numbers to define the propagation modes

$$m = 1 ; n = 0$$

a = waveguide width (m)

b = waveguide height (m)

The waveguide wave number (k_z) equation then becomes ^[1]

$$k_z = \sqrt{(k^2 - (\pi/a)^2)} \quad (5)$$

Where k = complex wave number of hydrocarbon

From this equation, we notice that the waveguide wave number is not related to the thickness of the hydrocarbon layer (omitted) and thus this method can be used to detect thin layer of hydrocarbon.

The refracted wave comes from the wave travels to the hydrocarbon layer. In order to get the wave propagation in the hydrocarbon layer, the wave must come in normal (perpendicular) to the hydrocarbon layer as can be seen in Figure 2. Thus, the refracted wave can be calculated with the equation provided below. ^[1]

$$V_{\text{refracted}} = A * e^{(j*2*k*d)} * e^{(j*k_z*\rho)} \quad (6)$$

Where A = antenna constant

k = complex wave number of the seabed

d = depth of the hydrocarbon layer from surface (m)

k_z = waveguide wave number of the hydrocarbon layer

ρ = distance between HED transmitter antenna to receiver antenna (m)

Here we notice that the refracted wave travels twice the distance between the seafloor and the seabed (d) and additional distance (ρ) inside the waveguide.

2.2 Electromagnetic Wave Scattering by Dielectric Cylinder of Arbitrary Cross Section Shape

Electromagnetic waves are waves belong to family of electromagnetic spectrum ranging from 1 Hz to 10^{23} Hz, sharing fundamental properties such as oscillating electric and magnetic field intensities at the same frequency.^[7] When an object is illuminated by a wave, a part of the incident power is scattered out and another part is absorbed by the object.^[8] Dielectric is material for which the valence band is completely filled and the energy gap is so great that free electrons are not normally available except under the application of extremely high energy.^[9] In other words, it acts as insulator or resistor, the opposite of a conductor. It has low conductivity (σ) while conductor has higher conductivity. Cylinder is a three dimensional shape which has two congruent circular bases in parallel planes which axis is perpendicular to the base.^[10] Cross section is the intersection of a body in 2-dimensional (or 3-dimensional) space with a plane.

The model to be tested in this project is taken from a journal of Jack H. Richmond (1963) "Scattering by a Dielectric Cylinder of Arbitrary Cross Section Shape".^[2] He stated that even though solutions are available for scattering by homogeneous dielectric cylinders of circular and elliptical cross section, only approximate solution existed for homogeneous or inhomogeneous cylinders of other shapes with finite cross section dimensions. A ray-optics technique was usually used by designers. Each ray passing through the dielectric body was assumed to undergo the same reflection and phase delay that was experienced by a plane wave passing through an infinitely wide plane sheet of the same thickness and with the same angle of incidence. This ray-optics method often provides reasonably accurate results for slightly curved dielectric shells, but it is inadequate for rapidly curving shells and the edge region of a truncated shell.

Richmond used integral equation technique for the field of a harmonic source in the presence of a dielectric cylinder of arbitrary cross section shape. The dielectric cylinder was divided into square cells which are small enough so that the electric field intensity was nearly uniform in each cell. The total electric field intensity within each cell was initially considered to be an unknown quantity. A

system of linear equations was obtained by enforcing at the center of each cell the condition that the total field must be equal to the sum of the incident and scattered fields. Richmond used digital computer to evaluate the electric field intensity in each cell. Below is the iteration of the technique. [2]

Consider a harmonic wave incident in free space on dielectric cylinder of arbitrary cross section as shown in Figure 3 below.

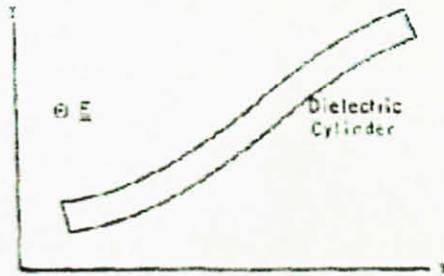


Figure 3. Cross section of a dielectric cylinder

- *) The incident electric field intensity has only z component, but not a function of z, where z axis is parallel with cylinder axis.

$$\mathbf{E}^i = z \mathbf{E}^i(x,y) \quad (7)$$

- *) The dielectric material is linear, meaning that every point in the dielectric reacts to the field in direct proportion to the field, and is isotropic, meaning that the interaction of the field with the dielectric is independent of the direction of that field, but may be inhomogeneous, meaning that every point in the dielectric reacts to the field in different way, with respect to the transverse coordinate. [11]

$$\epsilon = \epsilon(x,y) \quad (8)$$

where ϵ represents the complex permittivity of the dielectric.

- *) The dielectric cylinder is assumed to have the same permeability as free space ($\mu = \mu_0 = 4\pi \cdot 10^{-7} \text{ H/m}$).

$$\mathbf{E} = \mathbf{E}^i + \mathbf{E}^s \quad (9)$$

where E = total field = field set up by source in the presence of the dielectric cylinder.

E^i = incident field

E^s = scattered field, difference between the total field and the incident fields

*) Since E^i does only have z component, then E and E^s will have only z component.

*) E^s may be generated by an equivalent electric current, J , radiating in unbounded free space, known as polarization current.

$$\mathbf{J} = \mathbf{j} * \omega * (\epsilon - \epsilon_0) * \mathbf{E} \quad (10)$$

Where ω = angular frequency (rad/s) = $2\pi * \text{frequency}(\text{Hz})$

ϵ = permittivity of dielectric

ϵ_0 = permittivity of free space (vacuum) = $8.854 * 10^{-12}$ (F/m)

*) Field of an electric current filament $d\mathbf{I}$ parallel with z axis in free space

$$d\mathbf{E}^s = -z (\omega * \mu / 4) * H_0^{(2)}(k * \rho) d\mathbf{I} \quad (11)$$

where $H_0^{(2)}$ $k \rho$ = Hankel function of order zero

ρ = distance from current filament to observation point

$k = \omega \sqrt{\mu_0 * \epsilon_0} = 2\pi / \lambda$

λ = free space wave length

*) The increment of electric current which generates the scattered field

$$d\mathbf{I} = \mathbf{J} d\mathbf{S} = \mathbf{j} * \omega * (\epsilon - \epsilon_0) * \mathbf{E} d\mathbf{S} \quad (12)$$

where $d\mathbf{S}$ is the increment of surface area (x,y) on the cross section of dielectric cylinder.

*) Combining equation (11) and (12) to derive the next equation of scattered field:

$$dE^s = -z (\omega^* \mu / 4) * H_0^{(2)}(k * \rho) * j * \omega * (\epsilon - \epsilon_0) * E dS$$

$$E^s = (-j * \omega^2 * \mu / 4) \iint (\epsilon - \epsilon_0) * E(x', y') H_0^{(2)}(k * \rho) dx' dy'$$

If the complex relative dielectric constant $\epsilon_r = \epsilon / \epsilon_0$ then $(\epsilon - \epsilon_0) = \epsilon_0 (\epsilon_r - 1)$

We know that $k = \omega \sqrt{(\mu_0 * \epsilon_0)}$ and $\mu = \mu_0$, thus $k^2 = \omega^2 \mu_0 \epsilon_0$

Thus

$$E^s = (-j * k^2 / 4) \iint (\epsilon_r - 1) * E(x', y') H_0^{(2)}(k * \rho) dx' dy' \quad (13)$$

where

$$\rho = \sqrt{((x-x')^2 + (y-y')^2)} \quad (14)$$

(x, y) = coordinate of the observation point

(x', y') = coordinate of the source point

*) Equation (13) is valid for scattered field at any point inside or outside dielectric region (homogeneous). Combining equation (9) and (13) we get

$$E^i = E - E^s$$

$$E^i(x, y) = E(x, y) + (j * k^2 / 4) \iint (\epsilon_r - 1) * E(x', y') H_0^{(2)}(k * \rho) dx' dy' \quad (15)$$

*) Richmond divided the cross section of dielectric cylinder into cells sufficiently small that the dielectric constant and electric field intensity are constant over each cell, as shown in Figure 4 below.

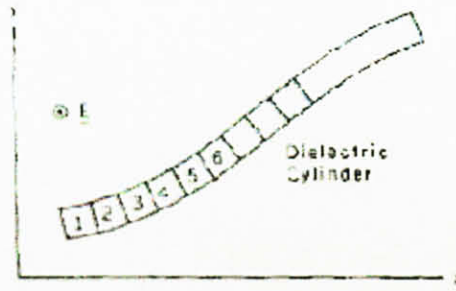


Figure 4. The cross section of the dielectric cylinder is divided into small cells.

*) Enforcing equation (12) at the center of cell m

$$\mathbf{E}_m^i = \mathbf{E}_m + (\mathbf{j} * \mathbf{k}^2 / 4) * \sum_{n=1}^N (\epsilon_n - 1) \mathbf{E}_n \iint_{\text{cell } n} \mathbf{H}_0^{(2)}(\mathbf{k} * \rho) dx' dy' \quad (16)$$

where

ϵ_n = complex relative dielectric constant at the center of cell n

E_n = electric field intensity at the center of cell n

$$\rho = \sqrt{((x' - x_m)^2 + (y' - y_m)^2)} \quad (17)$$

*) taking $m = 1, 2, 3, \dots, N$, equation (16) yields a system of N linear equations, where N = number of cells. These can be solved to determine the total electric field intensity at the center of each cell ($E_1, E_2, E_3, \dots, E_n$).

*) Having thus determined, the total electric field $E(x,y)$ in the dielectric region, it is then possible to calculate the scattered field of the dielectric cylinder at any point in space by using equation (13).

*) Trapezoidal rule and Simpson's rule can be used to evaluate surface integral in equation (16). It is quite lengthy, and careful calculation must be carried out in integrating through singularity that exists when the observation point is at the center of cell n. The region of integration (over cell n) is square or rectangular. Beside, the closed-form solution for this integral is not known.

*) Richmond proposed solution using the integral of zero-order Hankel function over a circular region, given by:

$$\begin{aligned}
 j^*k^2/4 * \int_0^{2\pi} \int_0^a (H_0^{(2)}(k^*\rho) \rho' d\rho d\phi') \\
 &= (j/2) [\pi^*k^*a^*H_1^{(2)}(k^*a) - 2j] \quad \text{if } m = n \\
 &= (j^*\pi^*k^*a/2) J_1(k^*a) H_0^{(2)}(k^*\rho_{mn}) \text{ if } m \neq n \quad (18)
 \end{aligned}$$

where ρ is given by equation (14) and ρ' and ϕ' are polar coordinates based on a coordinate origin at the center of cell n .

*) The first solution applies when the observation point is at the center of circular region while the second solution applies when the observation point is at a distance ρ_{mn} from the center of circular region where $\rho_{mn} > a$, radius of the circular region.

$$\rho_{mn} = \sqrt{(x_m - x_n)^2 + (y_m - y_n)^2} \quad (19)$$

*) Looking and replacing back equation (16)

$$E_m^i = \sum_{n=1}^N C_{mn} E_n \quad (20)$$

where $m = 1, 2, 3, \dots, N$

$$C_{mn} = 1 + (\epsilon_m - 1) (j/2) [\pi^*k^*a_m^*H_1^{(2)}(k^*a_m) - 2j], \quad \text{if } n = m \quad (21)$$

$$C_{mn} = (j^*\pi^*k^*a_n/2) (\epsilon_n - 1) J_1(k^*a_n) H_0^{(2)}(k^*\rho_{mn}), \quad \text{if } n \neq m \quad (22)$$

Here, Richmond proofed that the total of the field is the summation of the field in each cell. $E_m^i = \sum_{n=1}^N E_n$

*) Once equation (20) is solved, we can calculate the scattered field at any point in space using equation (13). Combining (13) and (18), and some part of (15), we would get:

$$E_s(x,y) = (-j\pi k/2) \sum_{n=1}^N (\epsilon_n - 1) E_n a_n J_1(k a_n) H_0^{(2)}(k \rho_n) \quad (23)$$

where

ϵ_n = average dielectric constant over cell n

a_n = radius of the circle having the same area as cell n

ρ_n = distance from the observation point to the center of cell n

$$\rho_n = \sqrt{(x - x_n)^2 + (y - y_n)^2} \quad (24)$$

*) Distant scattering pattern of the dielectric cylinder is obtained by employing the asymptotic form for the Hankel function of large argument.

$$\rho_n = \rho_0 - x_n \cos \varphi - y_n \sin \varphi \quad (25)$$

where ρ_0 and φ are polar coordinates of the distant observation point.

*) Then, the distant scattered field is given by equation below

$$E_s(\rho_0, \varphi) = (-j\pi k/2) \sqrt{2j/(\pi k \rho_0)} e^{(-j k \rho_0)} \sum_{n=1}^N (\epsilon_n - 1) E_n a_n J_1(k a_n) e^{(j k (x_n \cos \varphi + y_n \sin \varphi))} \quad (26)$$

*) plane wave scattering properties of any cylindrical body of infinite length are described in terms of the echo width ($W(\varphi)$)

$$W(\varphi) = \lim_{(\rho_0 \rightarrow \infty)} 2\pi \rho_0 |E^s(\rho_0, \varphi)|^2 / |E^i|^2 \quad (27)$$

*) Combining equation (26) and (27), the echo width of a dielectric cylinder of arbitrary cross section shape is given as

$$W(\varphi) = \pi^2 k / |E|^2 * |\sum_{n=1}^N (\epsilon_n - 1) E_n a_n J_1(k a_n) e^{j k (x_n \cos \varphi + y_n \sin \varphi)}|^2 \quad (28)$$

Solution of the wave scattered from the hydrocarbon layer is obtained by combining equation (13), (14), (18), and (19). The solution of the integration of Hankel function of order zero is provided in equation (18). From this equation, the value of m is taken not to be the same with the value of n and thus the second solution of equation (18) is used.

Hankel function is actually the third type of Bessel function, which consists the first and the second Bessel function ($J_\alpha(x)$ and $Y_\alpha(x)$ respectively).^[12] The zero order of the second type of Hankel function $H_0^{(2)}$ is formulated with the equation below.

$$H_0^{(2)} = J_0(x) - jY_0(x) \quad (29)$$

$$J_0(x) = 1/\pi * \int_0^\pi (\cos(-x \sin(\tau))) d\tau \quad (30)$$

$$= 1/2\pi * \int_{-\pi}^\pi (e^{-j(-x \sin(\tau))}) d\tau \quad (31)$$

$$Y_0(x) = (J_0(x) \cos(0 \cdot \pi) - J_{-0}(x)) / \sin(0 \cdot \pi) = 0/0 \quad (32)$$

Taking the limit of $Y_0(x) = \lim_{\alpha \rightarrow 0} (Y_\alpha(x))$

$$Y_0(x) = (J_0(x)' \cos(0) - J_0(x) \sin(0) - J_0(x)') / \cos(0) = 0/1 = 0 \quad (33)$$

Thus,

$$\begin{aligned} H_0^{(2)} &= 1/\pi * \int_0^\pi (\cos(-x \sin(\tau))) d\tau - 0 \\ &= 1/\pi * \int_0^\pi (\cos(-x \sin(\tau))) d\tau \end{aligned} \quad (34)$$

$$J_1(x) = 1/\pi * \int_0^\pi (\cos(\tau - x * \sin(\tau))) d\tau \quad (35)$$

$$= 1/2\pi * \int_{-\pi}^\pi (e^{-j*(\tau - x * \sin(\tau))}) d\tau \quad (36)$$

Rearranging the equation (13), (14), (18), (19), (34), and (36), the scattered field of the wave coming from the hydrocarbon layer is calculated with the equation below.

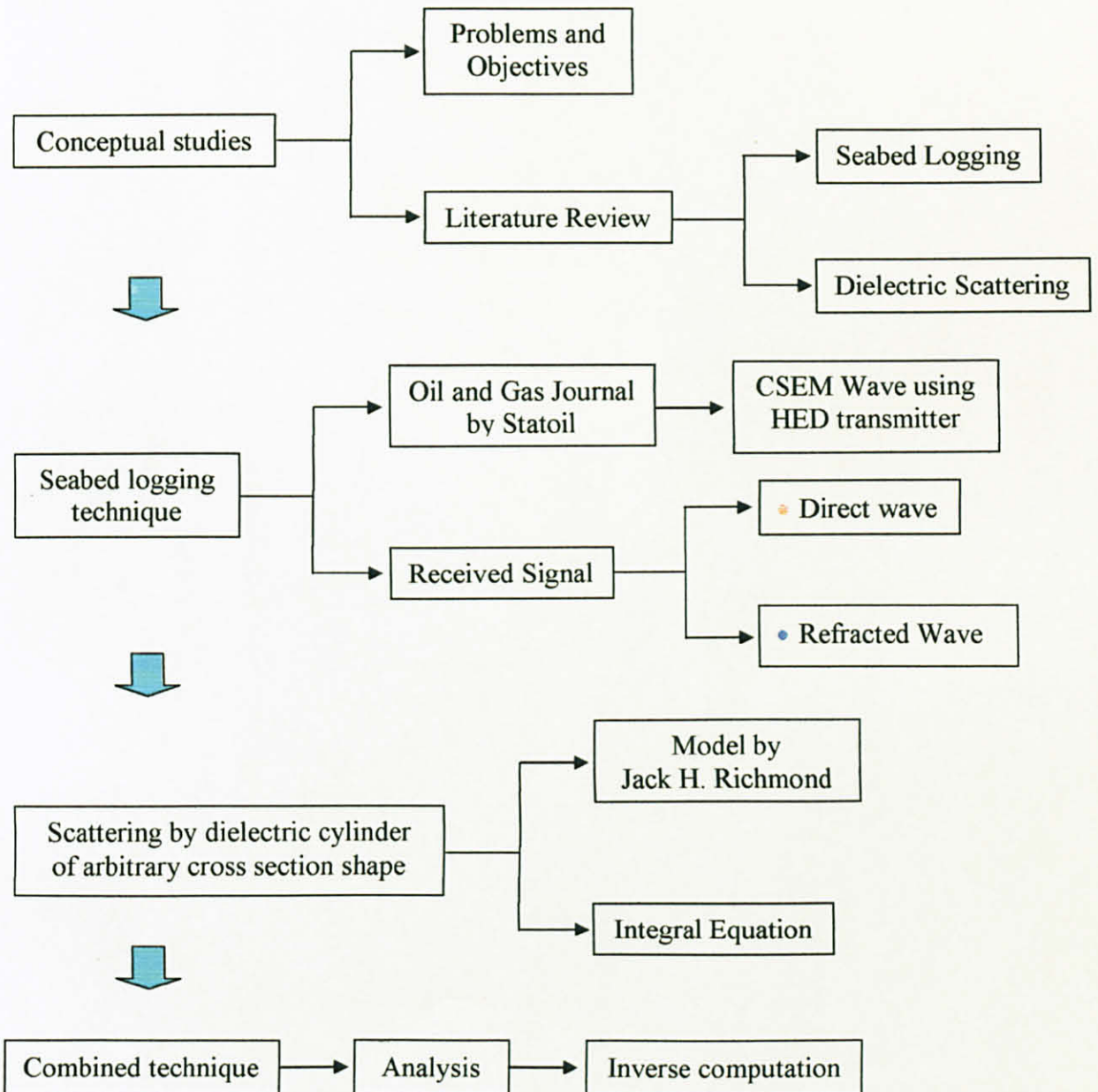
$$\begin{aligned} E^s &= (\epsilon_r - 1) * E(x', y') * (j * \pi * k * a / 2) * J_1(k * a) H_0^{(2)}(k * \rho_{mn}) \\ &= (\epsilon_r - 1) * E(x', y') * (j * \pi * k * a / 2) * 1/\pi * \int_0^\pi (\cos(\tau - (k * a) * \sin(\tau))) d\tau * \\ & \quad 1/\pi * \int_0^\pi (\cos(-x * \sin(\tau))) d\tau \end{aligned} \quad (37)$$

This technique is promising to give a better approximation to a dielectric material with arbitrary cross section shape. Thus, it can be applied in the seabed logging model to approximate the guided wave traveling through the hydrocarbon layer which is modeled as dielectric cylinder. Analyzing this wave combined with the direct wave would reveal the characteristics of the hydrocarbon reservoir underneath the seabed. This result is also compared with the Seabed Logging method that the Statoil provides as explained in previous section.

CHAPTER 3

METHODOLOGY

3.1 Project Flow Charts



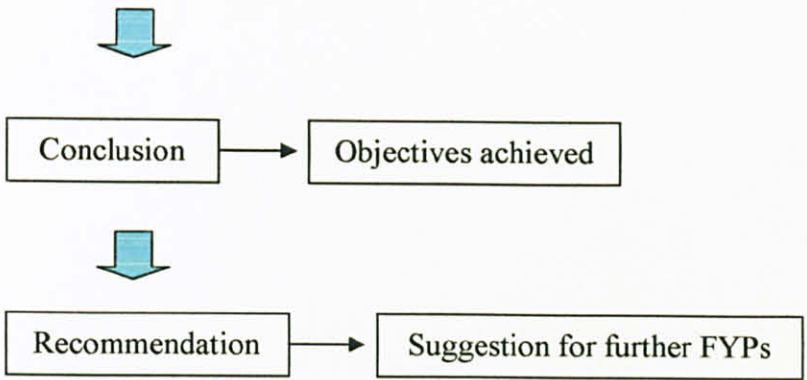


Figure 5. Flow chart of Final Year Project

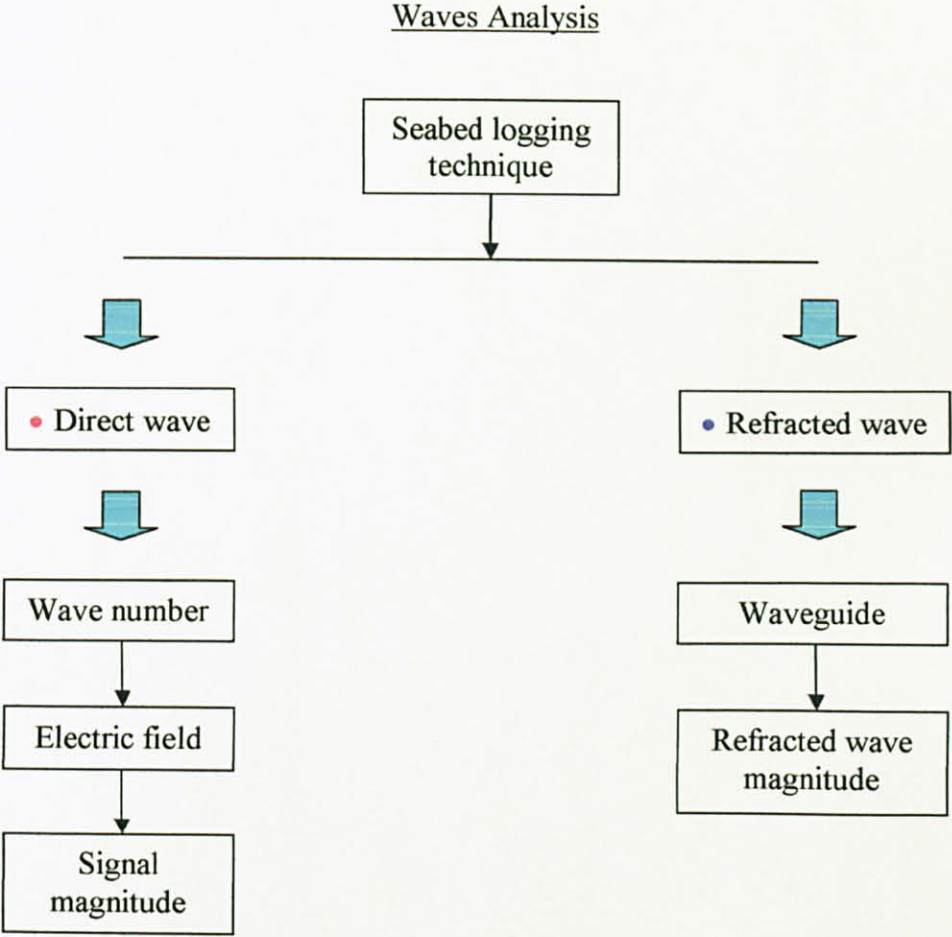


Figure 6. Flow chart of analysis of wave

Complex Waves Number

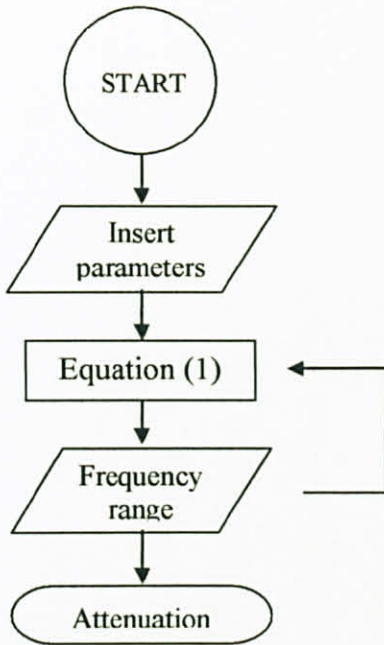


Figure 7. Flow chart of complex wave number

Electric Field

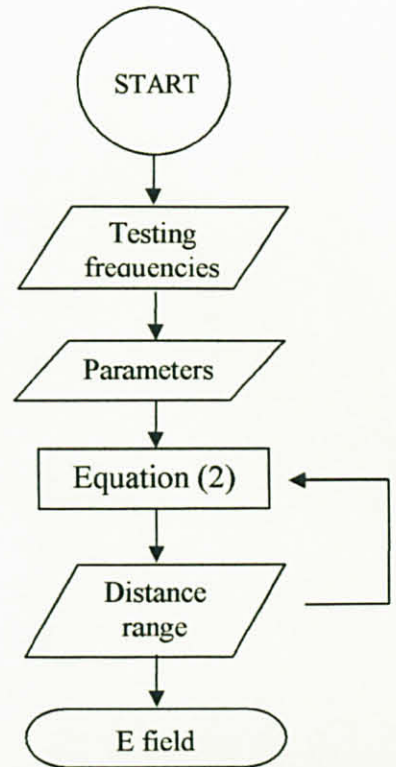


Figure 8. Flow chart of electrical field of direct wave

Signal Magnitude

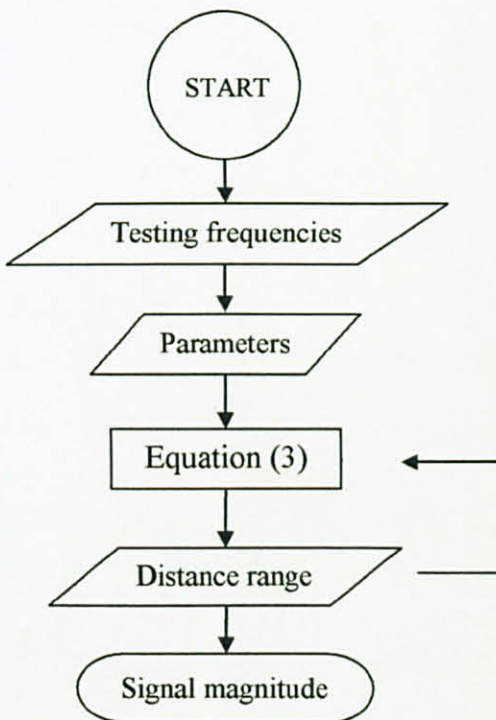


Figure 9. Flow chart of direct wave signal magnitude

Waveguide

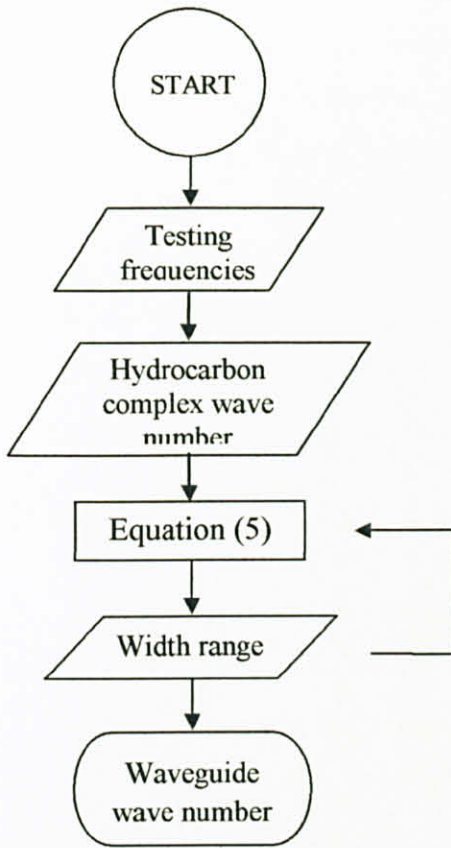


Figure 10. Flow chart of waveguide

Refracted Wave

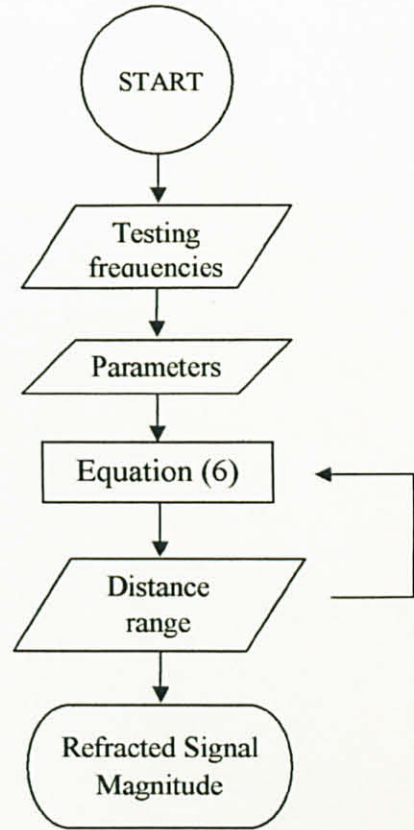


Figure 11. Flow chart of refracted signal

3.2 Procedure Identification

Conceptual studies consist of determining the problem that is faced and the objectives to achieve of the project. Literature review is done to widen the horizon of knowledge and sharpen the understanding of the background of the situation as well as to give some ideas of what people have done earlier in similar area. It gives ideas of possible method to solve the problem and achieve the objectives of the project.

As explained in previous chapters, this project aims to propose a way of seabed logging by combining the technique developed by Statoil and the model of scattering by dielectric cylinder of arbitrary cross section shape developed by Jack

H. Richmond, Kong F.N, et al from Statoil published a Journal in 2002 about the technique they used for seabed logging. The simulation was done in 3D and was tested off West Africa in 2000 and Norwegian Sea in 2001.^[1] They confirmed that the result was good proximity. In this project, their technique of modeling the complex wave number of the received wave directly from transmitter to receiver is used, to obtain the information of the characteristics of the direct wave. The Richmond's scattering by dielectric cylinder of arbitrary cross section shape technique is used to model the wave scattered from the hydrocarbon reservoir. The hydrocarbon layer is modeled as a shape of dielectric cylinder. Both techniques are then combined to analyze the result of this proposed Seabed Logging technique.

3.3 Tools and Equipments

The program is developed in MATLAB version 7.3.0.267 (R2006b). The code is written in C language and the function is initially built on the M-File Editor. To simulate the program, the function is called from the Command Window and the result is shown graphically on separated window. To edit the program or to vary the parameters with different range, one must go to the M-File Editor and directly edit the source code. The simulation result in this report is shown in graphical forms.

For further progress and presentation purpose, the program is developed and run in Graphical Users Interface (GUI) form. It enables users to run the program and change the parameter values directly on the provided windows, without having to deal directly with the source code. The simulation result is also shown in graphical forms.

CHAPTER 4

RESULTS AND DISCUSSION

4.1 Results

The frequency of EM wave is varied from 0.1 Hz to 50 Hz while the resistivity of both the overburden layer (R1) and the hydrocarbon layer (R2) are fixed at certain value. The overburden layer has resistivity $R = 1\Omega$ and permittivity $\epsilon = 20$ while the hydrocarbon has resistivity $R = 50\Omega$ and permittivity $\epsilon = 6$. Using the complex wave number equation (1), the attenuation constant is obtained as shown by the Figure 12 below.

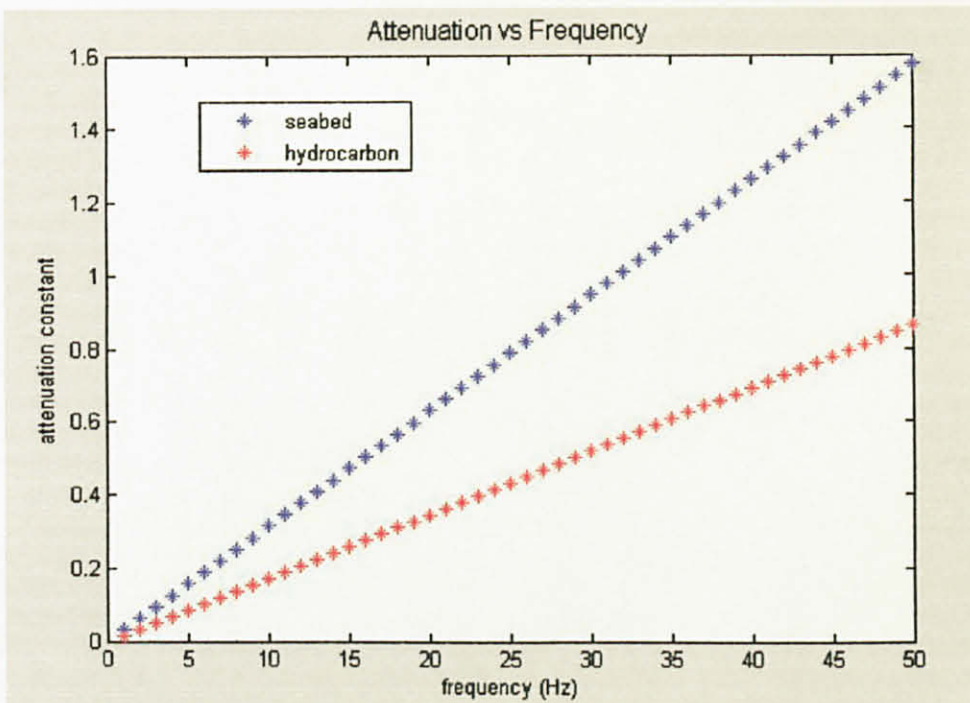


Figure 12. Attenuation versus frequency

Using equation (2), three values of transmitted EM wave frequency, 0.25 Hz, 1 Hz and 5 Hz are taken to measure the varied electric field in the sea water nearby the seabed surface, where the receiver antennas are installed. The transmitter current $I = 300$ A, the transmitter effective length $L_t = 100$ m, the complex wave number (of seabed) is taken at frequencies of 0.25 Hz, 1 Hz and 5 Hz (for testing and comparing purpose), the electric conductivity of the sea water $\sigma_{\text{sea}} = 4.8$ S/m (at average salinity of 35 g/Kg at about 20° C) and the distance between the HED transmitter antenna and the receiver antenna is initially varied from 0 to 150 meter. Figure 13 below shows the effect of the distance between the HED transmitter antenna and the receiver antenna with three different frequencies.

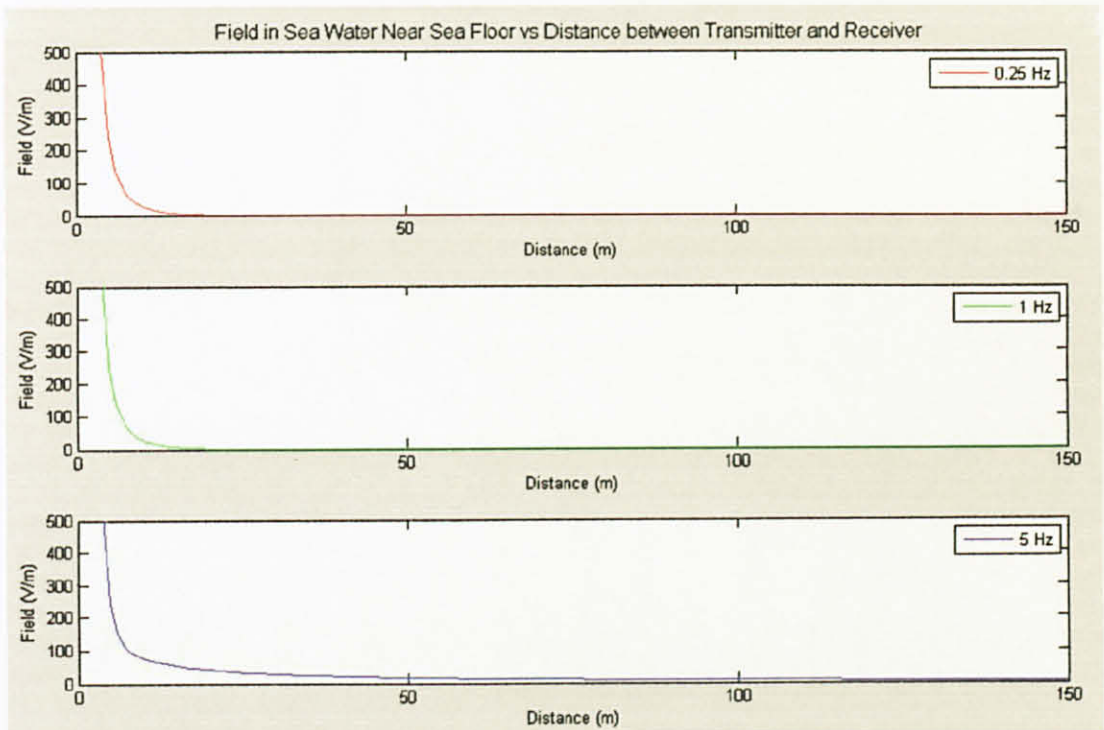


Figure 13. Electric field versus distance

Using equation (3), the signal magnitude received by a receiver antenna is measured also in three different values of transmitted EM wave frequency. The receiver effective length = 100 m. As the HED transmitter antenna moves, the radial distance between the transmitter antenna and the receiver antenna changes and it is simulated from 0 – 2000 meter. Figure 14 below shows the simulation result.

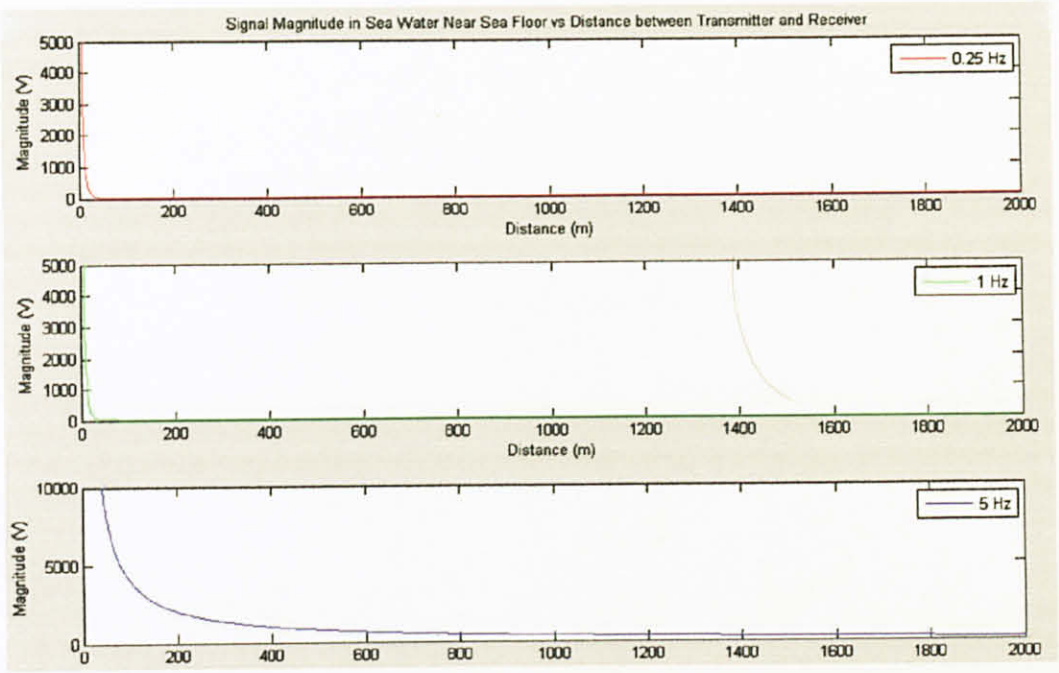


Figure 14. Magnitude of direct wave versus distance

The distance between the HED transmitter antenna and the receiver antenna is now fixed to 50 meter. The signal magnitude is then normalized with the value at 50 meter. The attenuation of the signal is shown by Figure 15 below.

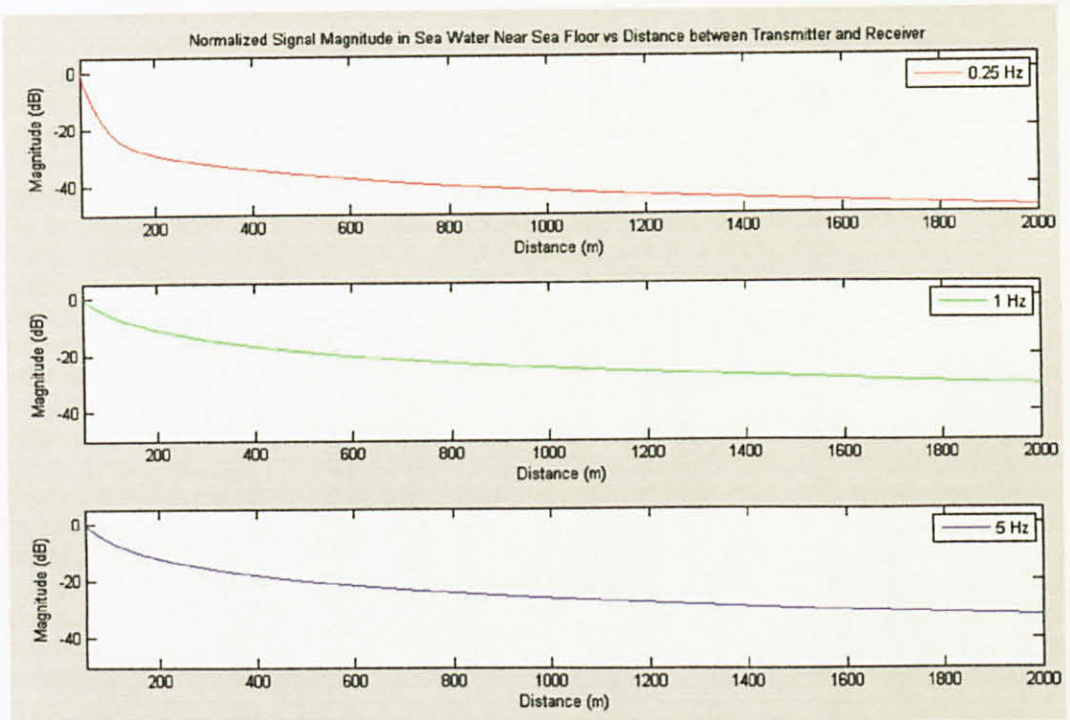


Figure 15. Direct wave attenuation

The refracted (or scattered) wave from the hydrocarbon layer is initially predicted using the waveguide wave number formula. Equation (5) is used because we would like to use this method in thin layer of hydrocarbon reservoir. Taking the hydrocarbon wave number from previous equation, the waveguide wave number is then calculated with the hydrocarbon reservoir width ranging from 0 – 1000 meter. The result shows the attenuation of the wave in the hydrocarbon layer at certain distance. Figure 16 below is the simulation result.

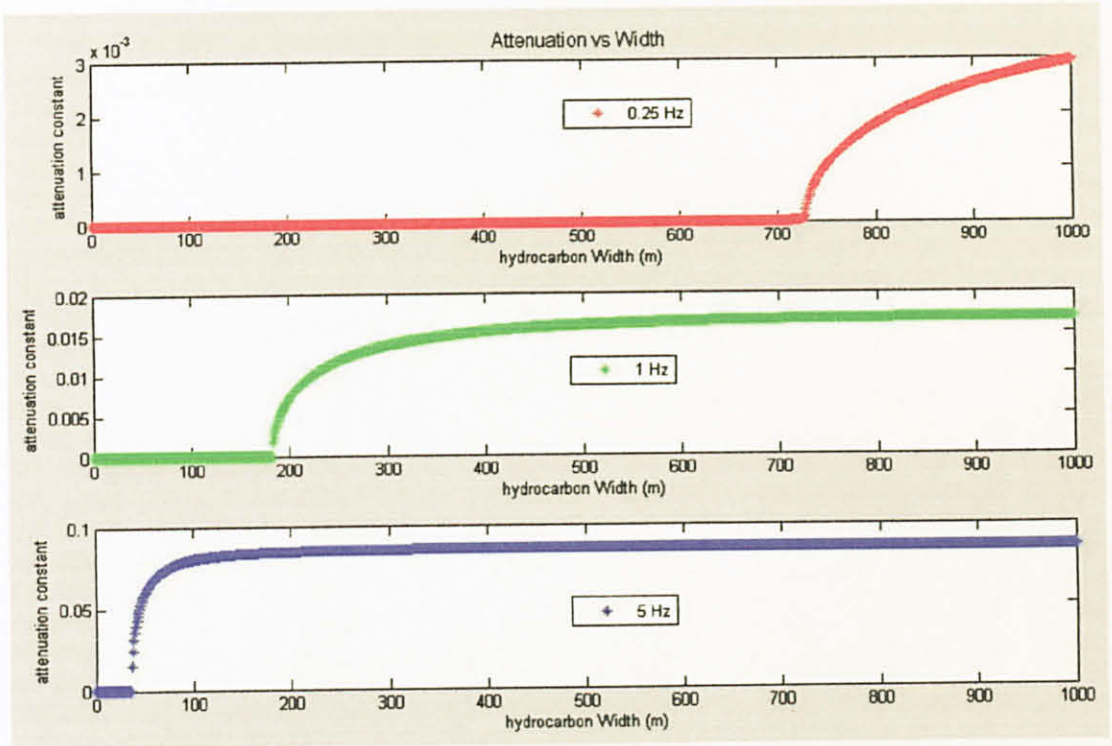


Figure 16. Waveguide wave number

Finally, the signal magnitude of the refracted wave from the hydrocarbon layer is calculated using equation (6). The hydrocarbon width is fixed at 1000 meter and the distance between the HED transmitter antenna and the receiver antenna is varied from 50 meter to 2000 meter. The result is normalized with the value at 50 meter. Figure 17 below shows the simulation result.

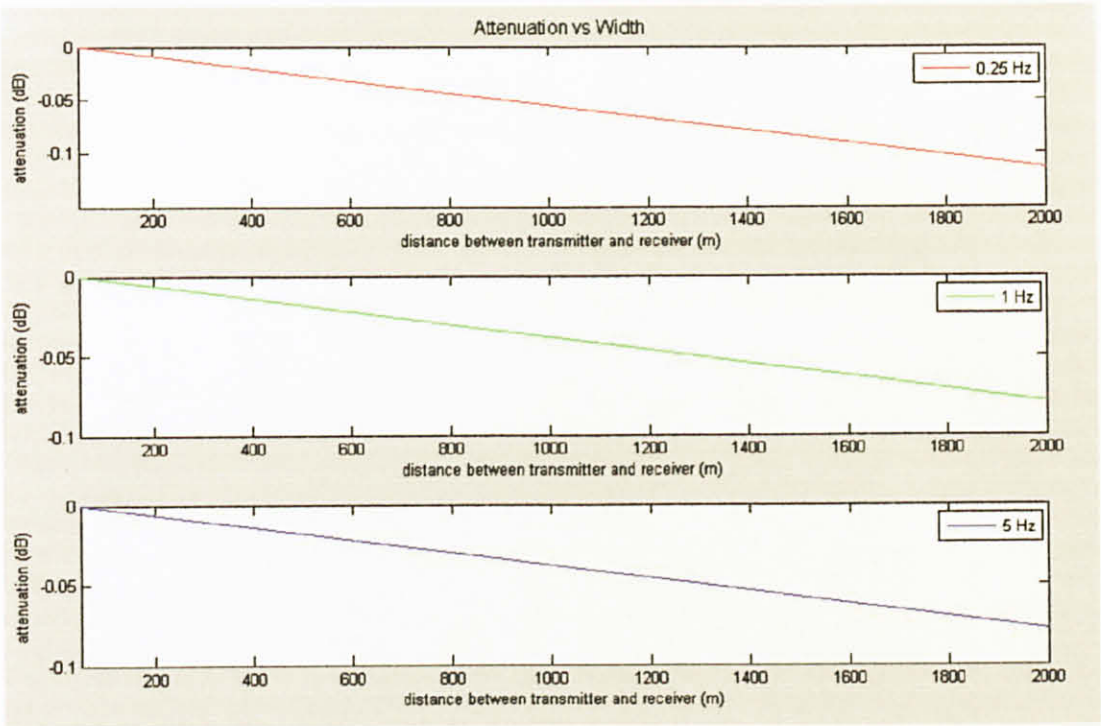


Figure 17. Refracted wave signal

4.2 Discussion

Figure 12 shows that the contrast resistivity levels of the hydrocarbon and the surrounding seabed give pretty much effect to the behavior of the EM wave attenuation. The signal which going through the seabed (lower resistivity) is attenuated higher than the signal going through the hydrocarbon layer (higher resistivity). Thus, the existence of hydrocarbon well beneath the seabed might be expected if the signal received shows attenuation contrast.

As the EM wave transmitted frequency gets higher, the contrast also gets clearer. The signal going through the seabed is much weaker than the signal going through hydrocarbon layer. However, the attenuation also gets higher. No signal might be received at all, neither from the seabed nor from the hydrocarbon layers. Thus, lower frequency is usually used in seabed logging technique to avoid high attenuation.

Figure 13 shows the usage of three different frequencies in measuring the electric field in the seawater nearby the sea floor. As the distance between the HED transmitter antenna and the receiver antenna gets further, the electric field gets lower. The challenge of using low frequency EM wave is that whether engineers would still be able to obtain data from weak signal. Low frequency means longer wave length. The signal might die out before it even reaches the receiver.

To overcome this, high current signal is used (here, $I = 300 \text{ A}$). The signal received is expected to be strong enough so that information would still be able to be extracted and analyzed. Figure 14 shows the signal magnitude received by the receiver antenna, at distance range form 0 to 2000 meter. When the HED transmitter antenna is close to the receiver antenna, the signal magnitude is really high and as it moves away, the magnitude fades out. It is necessary to set certain (minimum) distance between the HED transmitter antenna and the receiver antenna for two reasons: to avoid dominant strong direct wave from transmitter when the distance is close and to keep the magnitude strong enough when the distance is far away. In the simulation, the HED transmitter antenna is set to move at a distance of around 50 meters above the sea floor where the receiver antennas are installed. This is the reference point where we normalize other values to see the attenuations, as used in Figure 15.

Figure 16 from equation (5) and Figure 17 from equation (6) show the behavior of the refracted wave from the hydrocarbon layer. The attenuation of the refracted wave is much lower than the attenuation of the direct wave. This feature will be clearly seen if we combine Figure 15 and Figure 17, as shown by figure below.

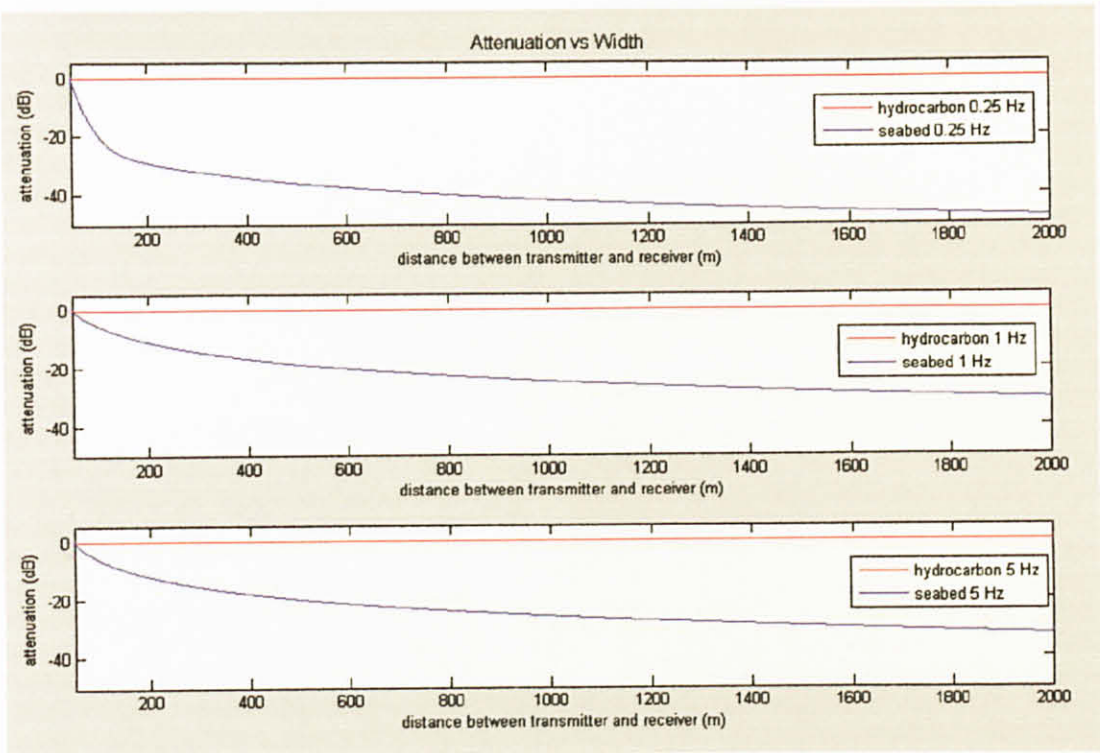


Figure 18. Contrast between direct and refracted waves

As clearly shown by Figure 18 above, the behavior of the direct wave contrasts the behavior of the refracted wave. When engineers find this characteristic, they might expect the presence of the hydrocarbon layer beneath the sea floor. In real practical works, it is very important to make sure the data obtained is valid and thus several experiment would be conducted. This data would then be combined with other data obtained with different approaches such as seismic data and the contents of the soil of the reservoir. Engineers would finally decide whether it is profitable to drill the well at that specified location. By accurately modeling the system and calculating the result, oil and gas companies would reduce the cost of drilling uneconomical dry well and thus the production cost would be reduced.

CHAPTER 5

CONCLUSION AND RECOMMENDATION

5.1 Conclusion

Seabed logging technique has recently been widely discussed and developed by oil and gas companies such as Shell and Statoil. It increases the possibility of predicting the presence of hydrocarbon reservoir and thus reduces the loss of drilling dry reservoirs. Thus, engineers and scientists try to come up with better and ideas and techniques. Mathematical models are used to approximate the system and to reduce costs as well as to avoid losses.

Engineers and scientists use the fact that the electrical resistivity of hydrocarbon reservoir is much higher than its surroundings to locate its presence underneath the seafloor. By sending low frequency EM wave from a HED transmitter antenna to the seabed and interpret data by analyzing the reflected wave received by receiver antennas installed on the seafloor, the information about the presence of the hydrocarbon could be obtained and further analyzed.

The signal received by the receivers mainly consists of two parts: the direct signal from the transmitter and the scattered signal from the hydrocarbon layer. The direct signal tells about the attenuation characteristics of the EM wave. The wave (signal) travels to the hydrocarbon layer is much stronger (less attenuated) than the one travels to the surrounding overburden area. This signal is analyzed to give information about the characteristics of the hydrocarbon reservoir.

Richmond provides the solution for scattering by dielectric cylinders with arbitrary cross section dimensions. This technique is used to analyze the wave going through the hydrocarbon (modeled by dielectric cylinder) and is very promising to give more precise approximation in modeling seabed logging. Combining this solution with the seabed logging technique, the presence of the hydrocarbon and its area could be more exactly predicted.

The contrast between the direct wave and the refracted (or scattered) wave promises the presence of hydrocarbon layer beneath the seabed. The attenuation of the refracted wave is much lower than the attenuation of the direct wave. Thus, engineers might expect the presence of the hydrocarbon layer beneath the sea floor once they find this characteristic on the data that they obtained. To support the decision, the data would then combined by other data obtained with other approaches. By accurately modeling the system and calculating the result, oil and gas companies would reduce the cost of drilling uneconomical dry well and thus the production cost would be reduced.

5.2 Recommendation

Graphical User Interface (GUI) should be developed for presentation and ease purposes. For further development and research, the author recommends using other models of scattering by dielectric cylinder. Using multi-layer dielectric cylinder scattering model might be a good approach. Besides, combining the technique with seismology mapping would be a valuable advantage to model the hydrocarbon reservoir in 3D. The result should then be compared to this one to contrast the preciseness of the solutions.

REFERENCES

- [1] Kong, F.N, et al. 2002, '*Seabed Logging*': *A possible direct hydrocarbon indicator for deepsea prospects using EM energy*. Oil and Gas Journal, May 2002.
- [2] Richmond, Jack H. 1963, *Scattering by a Dielectric Cylinder of Arbitrary Cross Section Shape*. IEEE Transactions on Antenna and Propagation, vol. AP-13, pp 334-341, May 1965.
- [3] Mehta, Kurang, etc. *Controlled Source Electromagnetic (CSEM) technique for detection and Delineation of hydrocarbon reservoirs*. Evaluation, University of British Columbia, Canada.
- [4] Guru, Bhag and Huseyin Hizirolu. 2004. *Electromagnetic Field Theory Fundamentals*. Second Ed. University Press, Cambridge.
- [5] Zitzewitz, Paul W. 1999, *Physics Principles and Problems*. McGraw Hill, USA.
- [6] Kong, J. A. 1986, *Electromagnetic Wave Theorys*. John Wiley & Sons.
- [7] Ulaby, Fawwaz T. 2005, *Electromagnetics for Engineers*. Pearson Education, Upper Saddle River.
- [8] Ishimaru, Akira. 1991, *Electromagnetic Wave Propagation, Radiation, and Scattering*. Prentice Hall, Upper Saddle River.
- [9] Paul, Clayton R, Keith W. Whites and Syed A. Nasar. 1998, *Introduction to Electromagnetic Fields*. Third Ed. McGraw Hill, USA.

- [10] Hoffer, Alan R. and Roberta Koss. 1998, *Focus On Geometry*. Addison Wesley Longman, Inc, USA.
- [11] Stewart, Joseph V. 2001, *Intermediate Electromagnetic Theory*. World Scientific, Singapore.
- [12] http://en.wikipedia.org/wiki/Bessel_function last retrieved on May 5, 2009 at 12.00 pm (GMT + 8)

APPENDICES

Wave number

```
function wavenum
```

```
% ***** operating frequency ***** %
f_max = 50; % max frequency (Hz) %
f = [1:1:f_max]; %
w = 2 * pi * f; %
% *****
% ***** defined parameters ***** %
u0 = 4 * pi * 10 ^ -7; % magnetic permeability %
% *****
% ***** overburden layer ***** %
ob_th = 1000; % overburden thickness (meter) %
ob_r = 1; % overburden resistivity (ohm meter) %
ob_e = 20; % overburden permittivity %
% *****
% ***** hydrocarbon layer ***** %
hc_th = 50; % hydrocarbon thickness (meter) %
hc_r = 50; % hydrocarbon resistivity (ohm meter) %
hc_e = 6; % hydrocarbon permittivity %
% *****
% ***** sea water ***** %
sea_dp = 1000; % sea depth (meter) %
sea_r = 0.2; % sea resistivity %
sea_s = 4.8; % sea electric conductivity (S/m) %
% *****

% ***** transmitter***** %
tr_lt = 100; % transmitter antenna effective length (meter)
tr_i = 300; % transmitter current (Ampere)
%
d_tr_ob = 50; % distance from transmitter antenna to seafloor
(meter) %
% *****

% ***** overburden wave number ***** %
ob_k = [];
n = 1;
while n <= f_max
    ob_k(n) = w(n) * sqrt((u0 * ob_e) + ((u0 * i) / (ob_r * w(n))));
    n = n + 1;
end

ob_k_real = real (ob_k);
ob_k_imag = imag (ob_k);
% ***** %
```

```

% ***** hydrocarbon wave number ***** %
hc_k = [];
n = 1;
while n <= f_max
    hc_k(n) = w(n) * sqrt((u0 * hc_e) + ((u0 * i) / (hc_r * w(n))));
    n = n + 1;
end
hc_k_real = real (hc_k);
hc_k_imag = imag (hc_k);
% ***** plotting ***** %
plot(f, ob_k_real, 'b*', f, hc_k_real, 'r*');
xlabel ('frequency (Hz)');
ylabel ('attenuation constant');
title ('Attenuation vs Frequency', 'FontSize', 12);
legend ('seabed', 'hydrocarbon');
axis([0 f_max 0 1.6]);
% ***** end of code ***** %

```

Electric Field

```

function field

% ***** operating frequency ***** %
f_max = 50; % max frequency (Hz) %
f = [1:1:f_max]; % %
w = 2 * pi * f; % %

% provide testing frequencies : 0.25 Hz, 1 Hz and 5 Hz %
w_eff1 = 0.25 * 2 * pi; % testing frequency 1 (rad/s) %
w_eff2 = 1 * 2 * pi; % testing frequency 2 (rad/s) %
w_eff3 = 5 * 2 * pi; % testing frequency 3 (rad/s) %
% ***** %

% ***** defined parameters ***** %
u0 = 4 * pi * 10 ^ -7; % magnetic permeability %
% ***** %
% ***** overburden layer ***** %
ob_th = 1000; % overburden thickness (meter) %
ob_r = 1; % overburden resistivity (ohm meter) %
ob_e = 20; % overburden permittivity %
% ***** %
% ***** hydrocarbon layer ***** %
hc_th = 50; % hydrocarbon thickness (meter) %
hc_r = 50; % hydrocarbon resistivity (ohm meter) %
hc_e = 6; % hydrocarbon permittivity %
% ***** %
% ***** sea water ***** %
sea_dp = 1000; % sea depth (meter) %
sea_r = 0.2; % sea resistivity %
sea_s = 4.8; % sea electric conductivity (S/m) %
% ***** %

% ***** transmitter antenna ***** %
tr_lt = 100; % transmitter antenna effective length (meter)
tr_i = 300; % transmitter current (Ampere)
d_tr_ob = 50; % distance from transmitter antenna to sea floor
              (meter)

```

```

% *****
% ***** overburden wave number ***** %
ob_k_eff1 = w_eff1 * sqrt((u0 * ob_e) + ((u0 * i) / (ob_r *
    w_eff1)));
ob_k_eff1_real = real (ob_k_eff1);
ob_k_eff1_imag = imag (ob_k_eff1);
ob_k_eff2 = w_eff2 * sqrt((u0 * ob_e) + ((u0 * i) / (ob_r *
    w_eff2)));
ob_k_eff2_real = real (ob_k_eff2);
ob_k_eff2_imag = imag (ob_k_eff2);
ob_k_eff3 = w_eff3 * sqrt((u0 * ob_e) + ((u0 * i) / (ob_r *
    w_eff3)));
ob_k_eff3_real = real (ob_k_eff3);
ob_k_eff3_imag = imag (ob_k_eff3);
% *****
% ***** 3 hydrocarbon wave numbers ***** %
hc_k_eff1 = w_eff1 * sqrt((u0 * hc_e) + ((u0 * i) / (hc_r *
    w_eff1)));
hc_k_eff2 = w_eff2 * sqrt((u0 * hc_e) + ((u0 * i) / (hc_r *
    w_eff2)));
hc_k_eff3 = w_eff3 * sqrt((u0 * hc_e) + ((u0 * i) / (hc_r *
    w_eff3)));
% *****
% Electric field in sea water near the sea floor %
E_tr_ob_eff1 = []; % at frequency = 0.25 Hz
E_tr_ob_eff2 = []; % at frequency = 1 Hz
E_tr_ob_eff3 = []; % at frequency = 5 Hz

n = 1;
d_max = 150; % max distance from antenna to receiver
d = [1:1:d_max];

while n <= d_max
    E_tr_ob_eff1(n) = tr_i * tr_lt * exp (ob_k_eff1_real) * ((n^-3)
        - (ob_k_eff1 * (n^-2) * i) -
        ((ob_k_eff1^2)/n));
    E_tr_ob_eff2(n) = tr_i * tr_lt * exp (ob_k_eff2_real) * ((n^-3)
        - (ob_k_eff2 * (n^-2) * i) -
        ((ob_k_eff2^2)/n));
    E_tr_ob_eff3(n) = tr_i * tr_lt * exp (ob_k_eff3_real) * ((n^-3)
        - (ob_k_eff3 * (n^-2) * i) -
        ((ob_k_eff3^2)/n));

    n = n + 1;
end

E_tr_ob_eff1_real = real (E_tr_ob_eff1);
E_tr_ob_eff1_imag = imag (E_tr_ob_eff1);
E_tr_ob_eff1_abs = abs (E_tr_ob_eff1);
E_tr_ob_eff1_angle = angle (E_tr_ob_eff1) * 180 / pi;
E_tr_ob_eff2_real = real (E_tr_ob_eff2);
E_tr_ob_eff2_imag = imag (E_tr_ob_eff2);
E_tr_ob_eff2_abs = abs (E_tr_ob_eff2);
E_tr_ob_eff2_angle = angle (E_tr_ob_eff2) * 180 / pi;
E_tr_ob_eff3_real = real (E_tr_ob_eff3);
E_tr_ob_eff3_imag = imag (E_tr_ob_eff3);
E_tr_ob_eff3_abs = abs (E_tr_ob_eff3);

```

```

E_tr_ob_eff3_angle = angle (E_tr_ob_eff3) * 180 / pi;
% *****

% ***** plotting *****

subplot (3,1,1);
plot(d, E_tr_ob_eff1_abs, 'r');
xlabel ('Distance (m)');
ylabel ('Field (V/m)');
title ('Field in Sea Water Near Sea Floor vs Distance between
Transmitter and Receiver', 'FontSize', 12);
legend ('0.25 Hz');
axis ([0 d_max 0 500]);

subplot (3,1,2);
plot(d, E_tr_ob_eff2_abs, 'g');
xlabel ('Distance (m)');
ylabel ('Field (V/m)');
legend ('1 Hz');
axis ([0 d_max 0 500]);

subplot (3,1,3);
plot(d, E_tr_ob_eff3_abs, 'b');
xlabel ('Distance (m)');
ylabel ('Field (V/m)');
legend ('5 Hz');
axis ([0 d_max 0 500]);

%***** end of code *****

```

Voltage (dB)

```

function voltagedb

% ***** operating frequency *****
f_max = 50; % max frequency (Hz)
f = [1:1:f_max];
w = 2 * pi * f;

% provide testing frequencies : 0.25 Hz, 1 Hz and 5 Hz
w_eff1 = 0.25 * 2 * pi; % testing frequency 1 (rad/s)
w_eff2 = 1 * 2 * pi; % testing frequency 2 (rad/s)
w_eff3 = 5 * 2 * pi; % testing frequency 3 (rad/s)
% *****

% ***** defined parameters *****
u0 = 4 * pi * 10 ^ -7; % magnetic permeability
% *****
% ***** overburden layer *****
ob_th = 1000; % overburden thickness (meter)
ob_r = 1; % overburden resistivity (ohm meter)
ob_e = 20; % overburden permittivity
% *****
% ***** hydrocarbon layer *****
hc_th = 50; % hydrocarbon thickness (meter)
hc_r = 50; % hydrocarbon resistivity (ohm meter)
hc_e = 6; % hydrocarbon permittivity
% *****

```

```

% ***** sea water ***** %
sea_dp = 1000; % sea depth (meter) %
sea_r = 0.2; % sea resistivity %
sea_s = 4.8; % sea electric conductivity (S/m) %
% ***** %

% ***** transmitter antenna ***** %
tr_lt = 100; % transmitter antenna effective length (meter)
tr_i = 300; % transmitter current (Ampere)
d_tr_ob = 50; % distance from transmitter antenna to sea floor(
meter)
% ***** %

% ***** receiver antenna ***** %
rc_lt = 100; % receiver antenna effective length (meter)
% ***** %

% ***** overburden wave number ***** %
ob_k_eff1 = w_eff1 * sqrt((u0 * ob_e) + ((u0 * i) / (ob_r *
w_eff1)));
ob_k_eff1_real = real (ob_k_eff1);
ob_k_eff1_imag = imag (ob_k_eff1);

ob_k_eff2 = w_eff2 * sqrt((u0 * ob_e) + ((u0 * i) / (ob_r *
w_eff2)));
ob_k_eff2_real = real (ob_k_eff2);
ob_k_eff2_imag = imag (ob_k_eff2);

ob_k_eff3 = w_eff3 * sqrt((u0 * ob_e) + ((u0 * i) / (ob_r *
w_eff3)));
ob_k_eff3_real = real (ob_k_eff3);
ob_k_eff3_imag = imag (ob_k_eff3);
% ***** %

% ***** 3 hydrocarbon wave numbers ***** %
hc_k_eff1 = w_eff1 * sqrt((u0 * hc_e) + ((u0 * i) / (hc_r *
w_eff1)));
hc_k_eff2 = w_eff2 * sqrt((u0 * hc_e) + ((u0 * i) / (hc_r *
w_eff2)));
hc_k_eff3 = w_eff3 * sqrt((u0 * hc_e) + ((u0 * i) / (hc_r *
w_eff3)));
% ***** %

% Signal Magnitude in sea water near the sea floor %
V_tr_ob_eff1 = []; % at frequency = 0.25 Hz
V_tr_ob_eff2 = []; % at frequency = 1 Hz
V_tr_ob_eff3 = []; % at frequency = 5 Hz

n = 1;
d_max = 2000; % max distance from antenna to receiver
d = [1:1:d_max];

while n <= d_max
    V_tr_ob_eff1(n) = tr_i * rc_lt * tr_lt * exp (ob_k_eff1_real) *
((n^-3) - (ob_k_eff1 * (n^-2) * i) -
((ob_k_eff1^2)/n));

```

```

V_tr_ob_eff2(n) = tr_i * rc_lt * tr_lt * exp (ob_k_eff2_real) *
((n^-3) - (ob_k_eff2 * (n^-2) * i) -
((ob_k_eff2^2)/n));
V_tr_ob_eff3(n) = tr_i * rc_lt * tr_lt * exp (ob_k_eff3_real) *
((n^-3) - (ob_k_eff3 * (n^-2) * i) -
((ob_k_eff3^2)/n));
n = n + 1;
end

V_tr_ob_eff1_real = real (V_tr_ob_eff1);
V_tr_ob_eff1_imag = imag (V_tr_ob_eff1);
V_tr_ob_eff1_abs = abs (V_tr_ob_eff1);
V_tr_ob_eff1_angle = angle (V_tr_ob_eff1) * 180 / pi;

V_tr_ob_eff2_real = real (V_tr_ob_eff2);
V_tr_ob_eff2_imag = imag (V_tr_ob_eff2);
V_tr_ob_eff2_abs = abs (V_tr_ob_eff2);
V_tr_ob_eff2_angle = angle (V_tr_ob_eff2) * 180 / pi;

V_tr_ob_eff3_real = real (V_tr_ob_eff3);
V_tr_ob_eff3_imag = imag (V_tr_ob_eff3);
V_tr_ob_eff3_abs = abs (V_tr_ob_eff3);
V_tr_ob_eff3_angle = angle (V_tr_ob_eff3) * 180 / pi;
% *****

% ***** plotting ***** %
V_eff1 = 20 * log10(V_tr_ob_eff1_abs / V_tr_ob_eff1_abs(50));
subplot (3,1,1);
plot(d, V_eff1, 'r');
xlabel ('Distance (m)');
ylabel ('Magnitude (dB)');
title ('Normalized Signal Magnitude in Sea Water Near Sea Floor vs
Distance between Transmitter and Receiver'); %
legend ('0.25 Hz');
axis ([50 d_max -50 5]);

V_eff2 = 20 * log10(V_tr_ob_eff2_abs / V_tr_ob_eff2_abs(50));
subplot (3,1,2);
plot(d, V_eff2, 'g');
xlabel ('Distance (m)');
ylabel ('Magnitude (dB)');
legend ('1 Hz');
axis ([50 d_max -50 5]);

V_eff3 = 20 * log10(V_tr_ob_eff3_abs / V_tr_ob_eff3_abs(50));
subplot (3,1,3);
plot(d, V_eff3, 'b');
xlabel ('Distance (m)');
ylabel ('Magnitude (dB)');
legend ('5 Hz');
axis ([50 d_max -50 5]);

% ***** end of code ***** %

```

Refracted Wave

```
function vrefrac

% ***** operating frequency ***** %
f_max = 50; % max frequency (Hz) %
f = [1:1:f_max]; % %
w = 2 * pi * f; % %

% provide testing frequencies : 0.25 Hz, 1 Hz and 5 Hz %
w_eff1 = 0.25 * 2 * pi; % testing frequency 1 (rad/s) %
w_eff2 = 1 * 2 * pi; % testing frequency 2 (rad/s) %
w_eff3 = 5 * 2 * pi; % testing frequency 3 (rad/s) %
% ***** %

% ***** defined parameters ***** %
u0 = 4 * pi * 10 ^ -7; % magnetic permeability %
% ***** %
% ***** overburden layer ***** %
ob_th = 1000; % overburden thickness (meter) %
ob_r = 1; % overburden resistivity (ohm meter) %
ob_e = 20; % overburden permittivity %
% ***** %
% ***** hydrocarbon layer ***** %
hc_th = 50; % hydrocarbon thickness (meter) %
hc_w_max = 1000; % hydrocarbon width (meter) %
hc_r = 50; % hydrocarbon resistivity (ohm meter) %
hc_e = 6; % hydrocarbon permittivity %
% ***** %
% ***** sea water ***** %
sea_dp = 1000; % sea depth (meter) %
sea_r = 0.2; % sea resistivity %
sea_s = 4.8; % sea electric conductivity (S/m) %
% ***** %

% ***** transmitter antenna ***** %
tr_lt = 100; % transmitter antenna effective length (meter)
tr_i = 300; % transmitter current (Ampere)
d_tr_ob = 50; % distance from transmitter antenna to sea floor(
    meter)
% ***** %

% ***** receiver antenna ***** %
rc_lt = 100; % receiver antenna effective length (meter)
% ***** %

% ***** 3 overburden wave numbers ***** %
ob_k_eff1 = w_eff1 * sqrt((u0 * ob_e) + ((u0 * i) / (ob_r *
    w_eff1)));
ob_k_eff1_real = real (ob_k_eff1);
ob_k_eff1_imag = imag (ob_k_eff1);

ob_k_eff2 = w_eff2 * sqrt((u0 * ob_e) + ((u0 * i) / (ob_r *
    w_eff2)));
ob_k_eff2_real = real (ob_k_eff2);
ob_k_eff2_imag = imag (ob_k_eff2);

ob_k_eff3 = w_eff3 * sqrt((u0 * ob_e) + ((u0 * i) / (ob_r *
    w_eff3)));
ob_k_eff3_real = real (ob_k_eff3);
```

```

ob_k_eff3_imag = imag (ob_k_eff3);
% *****

% ***** 3 hydrocarbon wave numbers ***** %
hc_k_eff1 = w_eff1 * sqrt((u0 * hc_e) + ((u0 * i) / (hc_r *
    w_eff1)));
hc_k_eff1_real = real (hc_k_eff1);
hc_k_eff1_imag = imag (hc_k_eff1);

hc_k_eff2 = w_eff2 * sqrt((u0 * hc_e) + ((u0 * i) / (hc_r *
    w_eff2)));
hc_k_eff2_real = real (hc_k_eff2);
hc_k_eff2_imag = imag (hc_k_eff2);

hc_k_eff3 = w_eff3 * sqrt((u0 * hc_e) + ((u0 * i) / (hc_r *
    w_eff3)));
hc_k_eff2_real = real (hc_k_eff2);
hc_k_eff2_imag = imag (hc_k_eff2);
% *****

% ** 3 hydrocarbon wave numbers in z direction ** %
hc_kz_eff1 = [];
hc_kz_eff2 = [];
hc_kz_eff3 = [];

n = 1;
hc_w_max = 1000; %maximum width of hydrocarbon layer
hc_wd = [1:1:hc_w_max];

while n<= hc_w_max
    hc_kz_eff1(n) = sqrt((hc_k_eff1 ^ 2) - ((pi/hc_wd(n))^2));
    hc_kz_eff2(n) = sqrt((hc_k_eff2 ^ 2) - ((pi/hc_wd(n))^2));
    hc_kz_eff3(n) = sqrt((hc_k_eff3 ^ 2) - ((pi/hc_wd(n))^2));
    n = n+1;
end

hc_kz_eff1_real = real (hc_kz_eff1);
hc_kz_eff1_imag = imag (hc_kz_eff1);
hc_kz_eff1_abs = abs (hc_kz_eff1);
hc_kz_eff1_angle = angle (hc_kz_eff1) * 180 / pi;

hc_kz_eff2_real = real (hc_kz_eff2);
hc_kz_eff2_imag = imag (hc_kz_eff2);
hc_kz_eff2_abs = abs (hc_kz_eff2);
hc_kz_eff2_angle = angle (hc_kz_eff2) * 180 / pi;

hc_kz_eff3_real = real (hc_kz_eff3);
hc_kz_eff3_imag = imag (hc_kz_eff3);
hc_kz_eff3_abs = abs (hc_kz_eff3);
hc_kz_eff3_angle = angle (hc_kz_eff3) * 180 / pi;
% *****

% **** refracted wave from hydrocarbon layer **** %
Vrefrac_eff1 = [];
Vrefrac_eff2 = [];

```

```

Vrefrac_eff3 = [];

hc_w_max = 1000; % hydrocarbon width (meter)
d_tr_ob = 2000; % distance from transmitter antenna to sea floor(
                meter)

n = 1;
m = 50;
distance = [m:1:d_tr_ob];

while m <= d_tr_ob
    Vrefrac_eff1(n) = exp(2*j*ob_k_eff1*hc_w_max) *
                    exp(j*hc_kz_eff1(1000)*distance(n)); %
    Vrefrac_eff2(n) = exp(2*j*ob_k_eff2*hc_w_max) *
                    exp(j*hc_kz_eff2(1000)*distance(n)); %
    Vrefrac_eff3(n) = exp(2*j*ob_k_eff3*hc_w_max) *
                    exp(j*hc_kz_eff3(1000)*distance(n)); %
    n = n+1;
    m = m+1;
end

Vrefrac_eff1_real = real (Vrefrac_eff1);
Vrefrac_eff1_imag = imag (Vrefrac_eff1);
Vrefrac_eff1_abs = abs (Vrefrac_eff1);
Vrefrac_eff1_angle = angle (Vrefrac_eff1);

Vrefrac_eff2_real = real (Vrefrac_eff2);
Vrefrac_eff2_imag = imag (Vrefrac_eff2);
Vrefrac_eff2_abs = abs (Vrefrac_eff2);
Vrefrac_eff2_angle = angle (Vrefrac_eff2);

Vrefrac_eff3_real = real (Vrefrac_eff3);
Vrefrac_eff3_imag = imag (Vrefrac_eff3);
Vrefrac_eff3_abs = abs (Vrefrac_eff3);
Vrefrac_eff3_angle = angle (Vrefrac_eff3);
%***** %

% ***** plotting ***** %
Veff1 = 20*log10(Vrefrac_eff1_abs/Vrefrac_eff1_abs(1));
subplot (3,1,1);
plot(distance, Veff1, 'r');
xlabel ('distance between transmitter and receiver (m)');
ylabel ('attenuation (dB)');
title ('Attenuation vs Width', 'FontSize', 12);
legend ('0.25 Hz');
axis ([50 d_tr_ob -0.15 0]);

Veff2 = 20*log10(Vrefrac_eff2_abs/Vrefrac_eff2_abs(1));
subplot (3,1,2);
plot(distance, Veff2, 'g');
xlabel ('distance between transmitter and receiver (m)');
ylabel ('attenuation (dB)');
legend ('1 Hz');
axis ([50 d_tr_ob -0.1 0]);

Veff3 = 20*log10(Vrefrac_eff3_abs/Vrefrac_eff3_abs(1));
subplot (3,1,3);
plot(distance, Veff3, 'b');
xlabel ('distance between transmitter and receiver (m)');

```

```
ylabel ('attenuation (dB)');  
legend ('5 Hz');  
axis ([50 d_tr_ob -0.1 0]);  
%*****gerhana 8771 - end of code ***** %
```

GUI for simulation

The screenshot shows a software window titled "SBL" with the main heading "SEABED LOGGING SIMULATION". The interface is organized into two columns. The left column contains parameter labels and their current values, while the right column contains buttons for simulation actions.

Parameter	Value	Action Button
Frequency range (Hz)	0 to 50	
Testing frequencies	0.1 Hz; 1 Hz; 5 Hz	
HC resistivity	50 ohms	Wave Number
HC permittivity	6	Direct Wave Field
HC depth	1000 m	
SB resistivity	1 ohm	Direct Wave Voltage
SB permittivity	20	
Transmitter current	300 A	Direct Wave Attenuation
Transmitter effective length	100 m	
Receiver effective length	100 m	Wave Guide
Distance between Transmitter and Receiver (m)	0 to 2000	
Sea water conductivity	4.8 S/m	Refracted Wave

Figure 19. GUI for Seabed Logging simulation